Selective Synthesis of Large Diameter, Highly Conductive and High Density Single-Walled Carbon Nanotubes by Thiophene-Assisted Chemical Vapor Deposition Method on Transparent Substrates†

Jinghua Li,‡[a] Keigo Otsuka,‡[a, b] Xiao Zhang,[a] Shigeo Maruyama,[b] and Jie Liu*[a]

[a] Department of Chemistry, Duke University, Durham, NC 27708, United States

Email: j.liu@duke.edu

[b] Department of Mechanical Engineering, the University of Tokyo, 7-3-1 Hongo, Bunkyo-ku, Tokyo 113-8656, Japan.

† Electronic supplementary information (ESI) available.

‡ J. L. and K. O. contributed equally to this work.

Abstract

Selective synthesis of single-walled carbon nanotubes (SWNTs) with controlled properties is an importance research topic for SWNT studies. Here we report a thiophene-assisted chemical vapor deposition (CVD) method to directly grow highly conductive SWNT thin films on substrates, including transparent ones. By adding low concentration thiophene into the carbon feedstock (ethanol), as-prepared carbon nanotubes demonstrates an obvious up-shift in the diameter distribution while the single-walled structure is still retained. In the proposed machanism, the change in the diameter is sourced from the increase in the carbon yield induced

by the sulfur-containing compound. Such SWNTs are found to possess high conductivity with 95% SWNTs demonstrating on/off ratios lower than 100 in transistors. More importantly, it is further demonstrated that this method can be used to directly synthesize dense SWNT networks on transparent substrates which can be utilized as transparent conductive films (TCFs) with very high transparency. Such TCFs can be applied to fabricate light modulating window as a proof-of-concept. The present work provides important insights into the growth mechanism of SWNTs and great potential for the preparation of TCFs with high scalability, easy operation and low cost.

Introduction

Single-walled carbon nanotubes (SWNTs) can be either semiconducting (s-) or metallic (m-) based on the electronic structure. S-SWNTs are highly attractive for logical gates, sensors and radio frequency devices because of the sizable energy band gap. In recent years, great progress has been made for the selective synthesis of s-SWNTs by the chemical vapor deposition (CVD) method.[1-10] On the other hand, SWNTs with metallic properties possess high conductivity, high transparency, and high flexibility, and therefore are promising candidates for the fabrication of transparent conductive films (TCFs) that can potentially compete with the indium tin oxide technology.[11]

However, one of the major drawbacks for SWNTs to serve as TCFs is that about 2/3 of them are semiconducting if we assume that SWNTs with different chiralities have equal opportunities to grow. To realize the application of SWNTs in TCFs, it is crucial to selectively prepare highly conductive SWNTs with metallic behavior since the conductivity of SWNT networks is limited by semiconducting pathways.[12] However, compared to the success in the selective synthesis of s-SWNTs, there are relatively fewer studies on how to grow SWNTs with metallic properties.[13-18] It is generally acknowledged that m-SWNTs are more reactive upon chemical etching because of the lower ionization potential, and the selective synthesis of s-SWNTs usually takes the advantage of the preferential removal of m-SWNTs.[19] As a result, the reliable and direct synthesis of highly conductive SWNT film with metallic behavior on target substrates remains challenging, and the growth mechanism is still not thorougly investigated. On the other hand, the deposition of presorted m-SWNT on substrates tends to form bundles and non-optimized junctions, reducing the overall conductivity and transmittance of the film.

In our earlier studies, it was found that the reactivity of m-SWNTs with chemical etchants is related to not only the electronic strcuture but also the diameter: in general, m-SWNTs with large diameters can be more stable than the small-diameter counterparts which have weaker sp^2 C-C bonding due to the larger curvature.[3] Additionally, earlier studies published by our group reported that in large-diameter range (>2.5 nm), m-SWNTs prefer to be nucleated during CVD synthesis with the detailed mechnism still not clear. However, these works pointed out one strategy to prepare highly conductive SWNTs by exploring ways to up-shift the diameter distribution. Previous studies show that the diameter and chirality distributions of SWNTs synthesized by CVD method are closely related to the growth conditions. For example, our group reported that under a fixed growth condition, only catalyst nanoparticles with the optimized size can be activated most effectively: smaller particles can be poisoned due to carbon overcoating, and larger particles are underfed for carbon nanotube nucleation.[20] Recently, it was also reported that sulfur-containing compounds can not only increase the yield of carbon nanotubes[21] but also induce SWNTs to alter towards different chiral species, double-walled carbon nanotubes (DWNTs), or multi-walled carbon nanotubes (MWNTs).[22-24] On the basis of these observations, we hypothesize that the introduction of sulfur-containing species into the synthesis system can result in the change of the growth atmophere and thus increase the average diameter of SWNTs in which SWNTs with metallic properties are the predominant species.

In this study, we present demonstration on the selective synthesis of large-diameter, highly conductive and high density SWNT networks by a thiophene-assisted CVD method. A small amount of thiophene is mixed with ethanol and acts together as the carbon feedstocks. It is found that the addition of thiophene leads to the shift of the diameter distribution towards larger values. Electrical measurement results show that as-prepared SWNTs contain ~95% nanotubes with an

on/off ratio smaller than 100 when fabricated into field effect transistors (FETs). It is further demonstrated that this approach can be applied to directly grow TCF on transparents substrates such as fused silica, which can be used for the fabrication of light modulating windows. This study provides a simple route for obtaining highly transparent and conductive SWNT films and may find broad application in TCF-based novel devices to benefit the general public.

Results and Discussion

To realize the role of the sulfur-containing compound during the synthesis of carbon nanotubes in our CVD method, different amounts of thiophene were mixed with ethanol and introduced as the carbon feedstocks through gas bubbling (see Experimental Section for details). Water vapor was also used during the CVD growth to reduce the amount of amorphous carbon in the sample and is also reported to extend the lifetime of the nanoparticles.[5] It was observed that even with ~0.1% thiophene, the side wall of the 1-inch quartz tube at the down stream of the gas flow turned black after growth (see Fig. S1 in Electronic Supplementary Material (ESI)), indicating that with the addition of thiophene, the growth system demonstrates a higher carbon decomposition rate than using pure ethanol. We found that the concentration of thiophene is the key factor influencing the type of carbon nanotubes produced: when the concentration is too low, it is not enough to induce obvious shift in the diameter distribution; on the other hand, an excessive amount of thiophene would result in the presence of double-walled and triple-walled carbon nanotubes as well as amophous carbons. Based on these observations, Fig. 1a schematically illustrates the proposed mechanism for the design of our experiment: a thin layer of sulfur coated onto the catalyst particles can promote the assembly of carbon atoms on the surface and thus increase the carbon yield.[22] The poisoning of nanoparticles smaller than the optimized size by excessive carbon feeding results in the deactivation of such particles for

carbon nanotube nucleation. Consequently, only nanotubes with larger diameters can be nucleated and elongated. Upon the test of different thiophene concentrations, an optimized growth condition was identified with the thiophene concentration of 0.1% (see Experimental Section for details). Fig. 1b shows a scanning electron microscope (SEM) image of the carbon nanotube networks on the SiO_2/Si substrate under this growth condition, and the density of the networks is significnatly higher than that of SWNTs prepared under the same condition but without thiophene (Fig. S2). Such carbon nanotubs were transferred onto copper grid for high-resolution transmission electron microscope (HRTEM) characterization, which confirms that as-prepared nanotubes are of large-diameter with the average diameter around 3.2 nm and retain the single-walled structure. Under the optimized thiophene concentration (0.1% in ethanol), no MWNTs are present as verified by TEM. However, if we continue increasing the concentration of thiophene (e.g. ~0.15%), some DWNTs begin to appear. Such SWNTs were characterized by Raman spectroscory, and the low intensity ratio of D band over G band in Raman sepectra verifies that these SWNTs are of high structural integrity (Fig. S3). In addition, unlike SWNTs prepared by our previously reported approaches,[3-5, 12, 25] the radial breathing mode (RBM) peaks in the low-frequency regime are rarely detected in the present experiments. That is consistent with the observation that as-synthesized SWNTs possess large diameter which leads to weak and unobservable RBM bands.

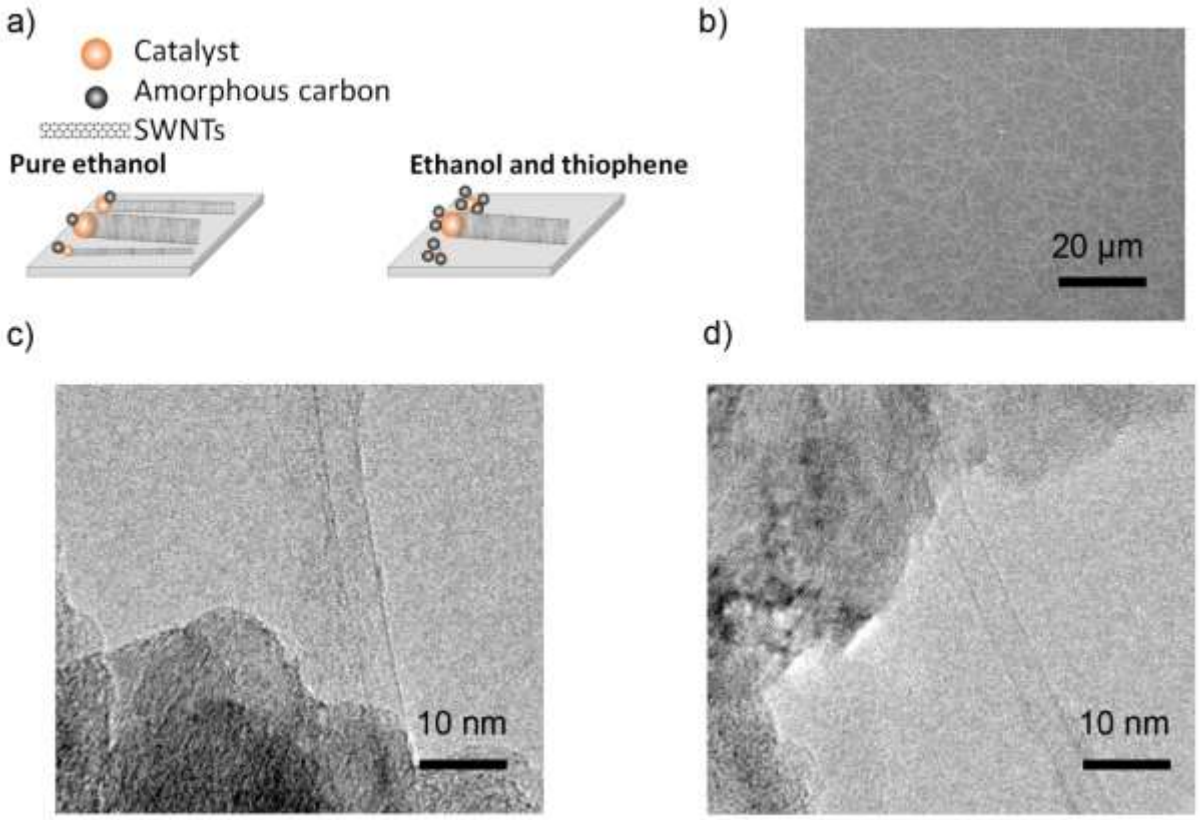

Fig. 1. (a) Schematic illustration showing the growth mechanism of the normal CVD method and our thiophene-assisted CVD method. (b) SEM image of as-prepared SWNT networks on SiO_2/Si substrate. (c, d) TEM images showing that carbon nanotubes synthesized by this method have large diameters and are single-walled.

In order to evaluate the selectivity of as-synthesized SWNTs, electrical measurements of FETs based on individual SWNTs were performed. Here a diluted catalyst concentration was used to avoid the formation of SWNT bundles which might introduce uncerntainty to the statistics. The device fabrication was directly conducted on the growth substrate with 280 nm SiO_2 as the dielectrics. Highly doped silicon was used for back-gating and the channel length was 2 μm. Fig. 2a shows the SEM image of a representative device. The transfer characteristics of the device is provided in Fig. 2b, and the on/off current ratio is estimated to be 1.2, indicating the metallic

property of the corresponding SWNT. Many devices were tested, and the histogram of the on/off ratios are plotted in Fig. 2c. Out of all the randomly selected SWNTs, 74% demonstrated on/off ratios lower than 10 and ~95% lower than 100. Previous studies by our group showed that a typical growth procedure using ethanol as the carbon feedstock usually leads to the ratio of m-SWNTs to be 33%.[5] Clearly, introducing thiophene into CVD synthesis results in the enrichment of SWNTs with metallic properties. A possible explanation for this phenomenon is that with increasing diameter, the sensitivity of m-SWNTs to oxidant (e.g. –OH groups in the carbon feedstock ethanol) will decrease due to the lower strain. At the same time, the larger diameter will lead to smaller band gaps of s-SWNTs and make them behave metallic at room temperature.

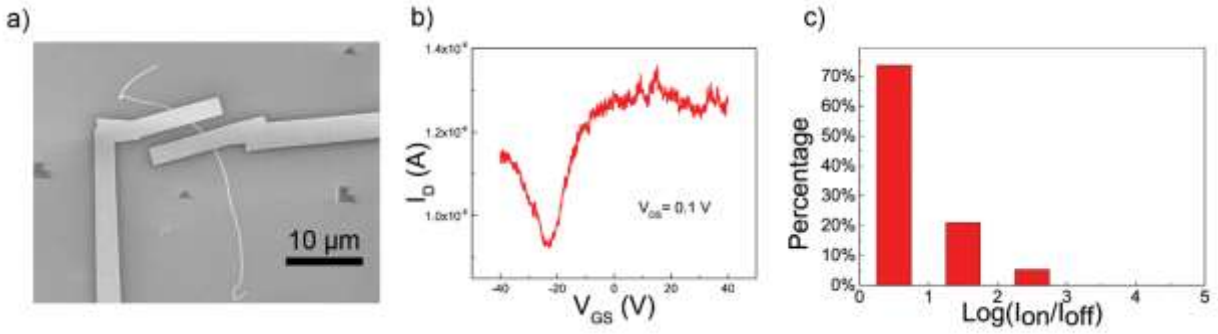

Fig. 2. (a) SEM image of a representative individual SWNT device. The channel length is 2 μm. (b) Transfer characteristics of an individual SWNT with the on/off ratio of 1.2 (V_{DS}= 0.1 V). (c) Histograms of on/off ratio of devices based on individual SWNTs synthesized with 0.1% thiophene.

To confirm our hyphothesis for the growth mechanism, atomic force microscope (AFM) was used to characterize the diameter distribution of these SWNTs. Fig. 3a shows the AFM image of a representative SWNT with the diameter of ~2.9 nm. It has been reported that SWNTs with the diameter above 2.5 nm tend to form flattened structure as a double layer graphene ribbon

analogue.[26, 27] To address this issue, we carefully examined the structure of as-prepared SWNTs by atomic AFM and TEM. We found that all the measured SWNTs prepared by the thiophene-assisted CVD method remain tubular. No signs of the occurrence of complete flattening were detected in our study. However, it is highly possible that the nanotubes are not perfectly circular and that could affect their electronic properties. The statistics of the diameter as a function of the on/off ratio of the corresonding SWNTs is plotted in Fig. 3b. It is found that all devices demonstrating on/off ratio between 1 to 2 contain nanotubes with the diamter larger than 2.5 nm. The bar chart in Fig. 3c demonstrates the diameter distribution upon the measurement of individual SWNTs by AFM, with the average and standard deviation of 3.2 and 1.0 nm, respectively. For comparison, the diameter distribution of SWNTs prepared under the same condition but without thiophene was also characterized, and the average and standard deviation are 1.43 and 0.34 nm (Fig. S4). In order to obtain information about the selectivity among more SWNTs, we further conducted electrical measurement on FETs based on multiple SWNTs. The SEM image of a representative device is shown in Fig. S5a. On the basis of the output characteristics of two test devices both containing 43 SWNTs prepared with (Fig. S5b, red) and without (Fig. S5b, black) 0.1% thiophene (the rest of the growth condition is the same), we found that the former group demonstrated a 70% lower resistance than the latter. By measuring more devices from both groups, the distributions of resistance per tube are shown in Fig. S5c and d. Note that the resistance value of the individual tube device includes both the resistance of the SWNTs and the resistance of the two metal-to-tube contacts. The average values are 360 and 710 kΩ per tube (including contact), respectively. Here we attribute the decrease in device resistance for SWNTs synthesized with thiophene to both the lower channel resistance and the lower contact resistance due to the increased ratio of SWNTs with metallic properties. According to

these electrical measurement results, we conclude that the thiophene-assisted CVD method leads to enriched amount of SWNT with metallic properties and therefore results in higher conductivity in the SWNT networks.

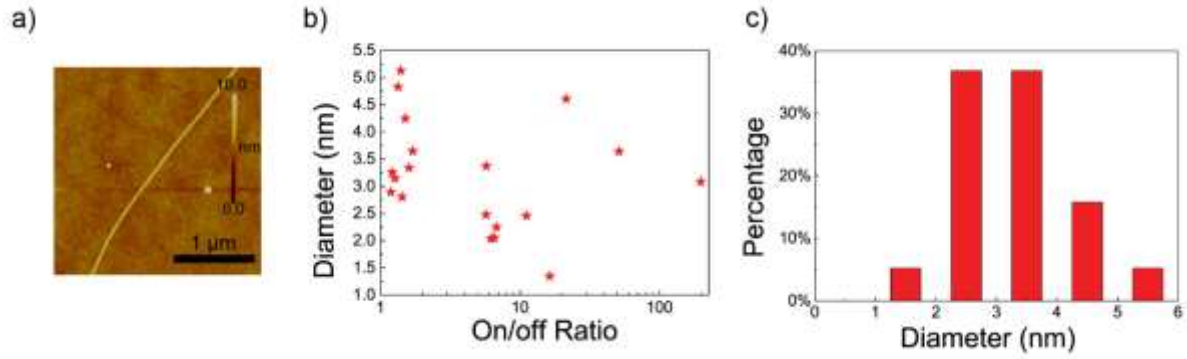

Fig. 3. (a) AFM image of an individual SWNT with the diameter of ~2.9 nm. (b) The diameters of SWNTs in Fig. 2c as a function of the on/off ratios. (c) Diameter distribution of SWNTs prepared by the thiophene-assisted CVD method. The average and standard deviation are 3.2 and 1.0 nm, respectively.

In addition, we consider the potential application of such highly conductive SWNT networks as TCFs. To achieve this goal, CVD growth was performed on highly transparent fused silica substrate. The previously reported multi-cycle growth method[25] was used in order to maximize the SWNT density, and here ethanol, methanol and thiophene together acted as the carbon feedstock (see Experimental Section for details). Fig. 4a shows the photograph of SWNT networks on the transparent substrate obtained by one-cycle, three-cycle and five-cycle growth, and the corresponding SEM images are provided in Fig. 4b, 4c and 4d, respectively. The sheet resistance of the networks was determined by the four-probe measurement. It was found that for samples with similar density, the sheet resistance changes from 249.2 to 52.6 kΩ/sq after adding thiophene (one growth cycle). Note that even though more amorphous carbons can be found on

the wall of the quartz tube when thiophene is used for the growth as mentioned above, we did not find large amount of amorphous carbons deposited onto the substrate and carbon nanotubes (where the temperature is much higher than the downstream of the quartz tube) than those obtained under the same growth condition but without thiophene, as verified by SEM, TEM and AFM. Therefore, it is believed that the conductivity difference is not affected by amorphous carbons. By enhancing the density of the networks using the multi-cycle growth, the sheet resistance can be further decreased to 24.0 kΩ/sq for three-cycle growth and 12.1 kΩ/sq for five-cycle growth, while the transmittance of the SWNT thin film can retain nearly 100% at the wavelength of 550 nm (Fig. S6).

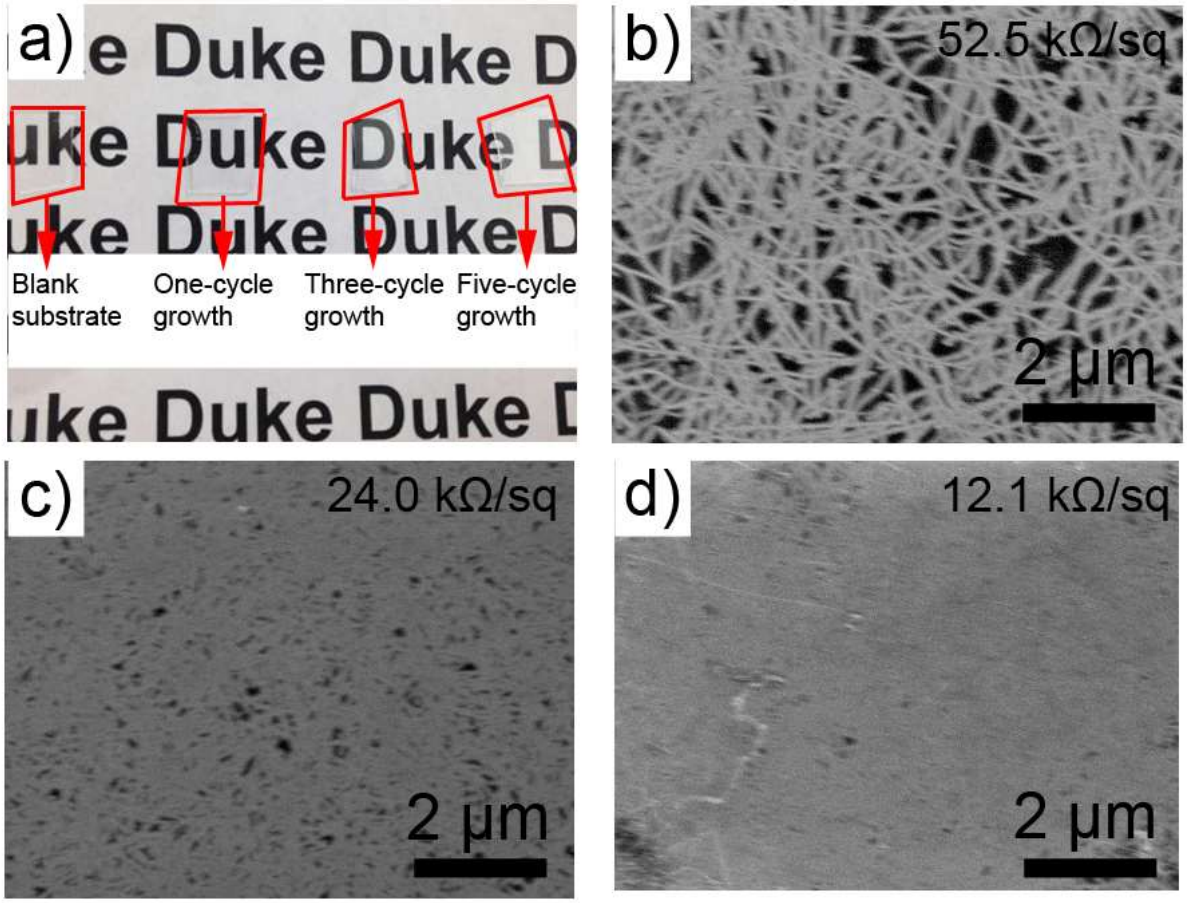

Fig. 4. (a) Photograph of a blank transparent fused silica substrate and SWNT random networks prepared by the multi-cycle growth method on substrates. (b-d) SEM images of SWNT random networks synthesized on fused silica substrates by the one-cycle (b), three-cycle (c), and five-cycle (d) growth method. The sheet resistances are 52.5, 24.0 and 12.1 kΩ/sq, respectively.

We further demonstrated the potential application of the highly conductive SWNT thin films by fabricating thermal-driven light modulating windows. Hydroxypropyl methyl cellulose (HPMC)-based hydrogel was employed to control the transmittance of the window.[28] The hydrogel is transparent under room temperature (22 ˚C), and reversibly turns into paper-white with low transmittance at a higher temperature (> 33 ˚C). The fabrication procedure is described in details in the Experimental Section. Briefly, the hydrogel was sealed between a glass slide and a conductive SWNT film on the transparent substrate, which simply serves as a heater upon voltage application. The design of the device is schematically illustrated in Fig. 5a. Fig. 5b shows the photographs of the window in the initial (transparent) state and in the final (paper-white) state due to the current-induced Joule heating when 80 V was applied (also see Video S1 in ESI). The window returned to the initial state soon after Joule heating stopped. The switching process was repeated under different bias voltages, and the light modulating window based on conductive SWNT films worked reversibly and stably. Switching time from the initial state to the final state decreased with an increasing applied voltage (Fig. 5c). The conductive SWNT networks were stable even with high voltage (~100 V) and showed constant resistance.

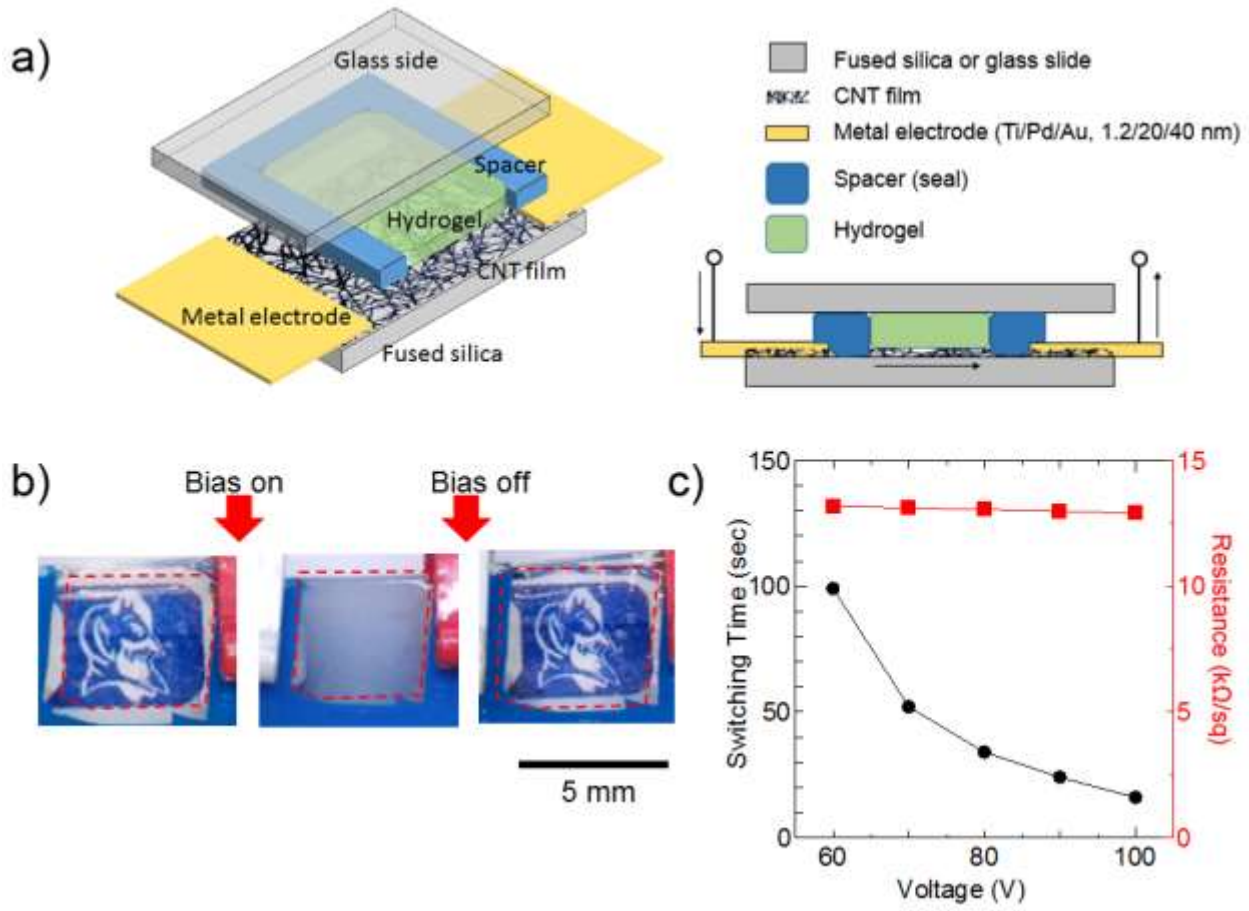

Fig. 5. (a) Schematic illustrations of the design of the light modulating window based on the highly conductive SWNT film on the transparent substrate (top view and side view). (b) Photographs showing the reversible color change from transparent to translucent when a bias voltage (80 V) was added. (c) Switching time and sheet resistance after the application of the bias as a function of the voltage.

Conclusion

To summarize, we demonstrated a thiophene-assisted CVD method to selectively synthesize highly conductive SWNTs with metallic behavior on target substrates. It was found that the diameter distribution can be effectively up-shifted by adding sulfur-containing compound into

the carbon feedstock. Under the optimized growth condition, carbon nanotubes with high conductivity can be obtained, which are confirmed to be single-walled and have large diameter. Based on the electrical measurement results, the ratio of SWNTs with on/off ratios lower than 100 is estimated to be ~95%. It was further shown that such a method can be applied for the direct growth of large diameter, highly conductive and high density SWNTs on transparent fused silica substrate to fabricate TCFs for broad applications, such as light modulating windows. Such SWNT thin films may find great potential in the development of transparent conductive devices with excellent performances.

Acknowledgements

This work was supported by the grant from National Science Foundation (CHE-1213469). The authors also acknowledge Duke SMiF (Shared Materials Instrumentation Facilities) for providing the instrumentation. K. O. is also supported by the global leader program for social design and management from University of Tokyo.

Experimental Section

Thiophene-assisted CVD method

The growth substrate (SiO_2/Si and fused silica) was cleaned by being treated with boiling H_2SO_4/H_2O_2 (2:1) solution for 0.5 h. $FeCl_3$ was dissolved in 10 mL ethanol to form 0.1 mmol/L solution as the catalyst precursor and spin-coated onto the substrate at the speed of 4000 rpm. For the growth of individual SWNTs with lower density for electrical measurement, the catalyst precursor solution was further diluted by 10 times.

The substrates with catalysts precursors were annealed in the air at 750 °C in the 1-inch Linderberg furnace for 15 min before cooling down to room temperature. Then the furnace was

heated up to 900 °C, and the catalysts precursors were reduced under a H_2 flow at 367 sccm for 3 min. For a typical CVD growth process, a H_2 flow at 130 sccm, an Ar flow at 81 sccm through an ethanol bubbler containing 0.1% thiophene and another Ar flow at 30 sccm through a water bubbler were introduced to the system. The bubblers were kept in a mixture of ice and water to maintain a constant temperature around 0 °C. The growth lasted for 15 min at 900 °C. The system was cooled down to room temperature with the protection of H_2. For the control group, a pure ethanol bubbler without thiophene was used instead with the rest conditions being the same.

For the growth of denser SWNTs for the preparation of light modulating window, a methanol bubbler was used instead of the water bubbler, and the Ar flow rate was 326 sccm. The multi-cycle growth strategy previously reported by our group[25] was applied to repetitively increase the density of SWNT networks. Transparent fused silica substrate was used for growth.

Characterization

A scanning electron microscope (SEM, FEI XL30 S-FEG, operated at 1.0 kV), an atomic force microscope (AFM, Digital Instruments Multiple Mode SPM Nanoscope IIIa, operated at tapping-mode) and a high-resolution transmission electron microscope (HRTEM, Tecnai F20 FEG-TEM, operated at 200 kV) were used for the characterization of SWNTs synthesized. The electrical measurement was performed by a Keithley 4200-SCS semiconductor characterization system. The sheet resistance of SWNT networks was measured by a Keithley four-probe station.

FET Fabrication

Back-gate FETs were fabricated on Si substrate having 280 nm SiO_2 as the dielectrics and the highly doped Si was used for gating. Electron-beam lithography (EBL) was used to pattern the electrodes with the channel length of 2 μm. Then Ti (1.2 nm)/Pd (20 nm)/Au (40 nm) were

deposited by electron-beam evaporation. After that, another lithography process followed by O_2 plasma exposure was conducted to remove SWNTs that bridged the electrodes outside of the channel area.

Light modulating window fabrication

A hydrogel composed of distilled water, HPMC, and sodium chloride (100/2/5 *w*/*w*/*w*) was used to switch the transmittance of the light modulating window. Ti (1.2 nm)/Pd (20 nm)/Au (40 nm) were deposited on the both ends of highly conductive SWNT films on the transparent fused silica substrate as the metal contact, leaving a small open window (~8 × 8 mm) in the middle. The sheet resistance of the SWNT thin film was ~13 kΩ/sq. The hydrogel was put between the transparent fused silica substrate and a bare glass slide. A spacer (blue in Fig. 5a) was used to keep the uniform thickness of the hydrogel and to avoid contact between the hydrogel and metal electrodes. The SWNTs and the metal electrodes were separated from the hydrogel by using poly(methyl methacrylate) and polyethylene films to avoid bubble formations and damages on SWNTs due to electrochemical reactions.

References

1. Y. C. Che, C. Wang, J. Liu, B. L. Liu, X. Lin, J. Parker, C. Beasley, H. S. P. Wong and C. W. Zhou, *ACS Nano*, 2012, **6**, 7454-7462.
2. L. Ding, A. Tselev, J. Y. Wang, D. N. Yuan, H. B. Chu, T. P. McNicholas, Y. Li and J. Liu, *Nano Lett.*, 2009, **9**, 800-805.
3. J. H. Li, C. T. Ke, K. H. Liu, P. Li, S. H. Liang, G. Finkelstein, F. Wang and J. Liu, *ACS Nano*, 2014, **8**, 8564-8572.
4. J. H. Li, K. H. Liu, S. B. Liang, W. W. Zhou, M. Pierce, F. Wang, L. M. Peng and J. Liu, *ACS Nano*, 2013, **8**, 554-562.
5. W. W. Zhou, S. T. Zhan, L. Ding and J. Liu, *J. Am. Chem. Soc.*, 2012, **134**, 14019-14026.
6. X. J. Qin, F. Peng, F. Yang, X. H. He, H. X. Huang, D. Luo, J. Yang, S. Wang, H. C. Liu, L. M. Peng and Y. Li, *Nano Lett.*, 2014, **14**, 512-517.
7. B. L. Liu, J. Liu, H. B. Li, R. Bhola, E. A. Jackson, L. T. Scott, A. Page, S. Irle, K. Morokuma and C. W. Zhou, *Nano Lett.*, 2015, **15**, 586-595.
8. S. S. Li, C. Liu, P. X. Hou, D. M. Sun and H. M. Cheng, *ACS Nano*, 2012, **6**, 9657-9661.
9. G. Hong, B. Zhang, B. H. Peng, J. Zhang, W. M. Choi, J. Y. Choi, J. M. Kim and Z. F. Liu, *J. Am. Chem. Soc.*, 2009, **131**, 14642-14643.
10. L. X. Kang, Y. Hu, L. L. Liu, J. X. Wu, S. C. Zhang, Q. C. Zhao, F. Ding, Q. W. Li and J. Zhang, *Nano Lett.*, 2015, **15**, 403-409.
11. A. Kumar and C. W. Zhou, *ACS Nano*, 2010, **4**, 11-14.
12. J. H. Li, A. D. Franklin and J. Liu, *Nano Lett.*, 2015, **15**, 6058-6065.
13. P. X. Hou, W. S. Li, S. Y. Zhao, G. X. Li, C. Shi, C. Liu and H. M. Cheng, *ACS Nano*, 2014, **8**, 7156-7162.

14. F. Yang, X. Wang, D. Q. Zhang, J. Yang, D. Luo, Z. W. Xu, J. K. Wei, J. Q. Wang, Z. Xu, F. Peng, X. M. Li, R. M. Li, Y. L. Li, M. H. Li, X. D. Bai, F. Ding and Y. Li, *Nature*, 2014, **510**, 522-524.

15. A. R. Harutyunyan, G. G. Chen, T. M. Paronyan, E. M. Pigos, O. A. Kuznetsov, K. Hewaparakrama, S. M. Kim, D. Zakharov, E. A. Stach and G. U. Sumanasekera, *Science*, 2009, **326**, 116-120.

16. B. H. Peng, S. Jiang, Y. Y. Zhang and J. Zhang, *Carbon*, 2011, **49**, 2555-2560.

17. R. Voggu, S. Ghosh, A. Govindaraj and C. N. R. Rao, *J. Nanosci. Nanotechnol.*, 2010, **10**, 4102-4108.

18. Y. Wang, Y. Q. Liu, X. L. Li, L. C. Cao, D. C. Wei, H. L. Zhang, D. C. Shi, G. Yu, H. Kajiura and Y. M. Li, *Small*, 2007, **3**, 1486-1490.

19. B. Yu, C. Liu, P. X. Hou, Y. Tian, S. S. Li, B. L. Liu, F. Li, E. I. Kauppinen and H. M. Cheng, *J. Am. Chem. Soc.*, 2011, **133**, 5232-5235.

20. C. G. Lu and J. Liu, *J. Phys. Chem. B*, 2006, **110**, 20254-20257.

21. T. P. McNicholas, L. Ding, D. N. Yuan and J. Liu, *Nano Lett.*, 2009, **9**, 3646-3650.

22. Y. Yuan, L. Wei, W. C. Jiang, K. Goh, R. R. Jiang, R. Lau and Y. Chen, *J. Mater. Chem. A*, 2015, **3**, 3310-3319.

23. W. C. Ren and H. M. Cheng, *J. Phys. Chem. B*, 2005, **109**, 7169-7173.

24. Z. P. Zhou, L. J. Ci, L. Song, X. Q. Yan, D. F. Liu, H. J. Yuan, Y. Gao, J. X. Wang, L. F. Liu, W. Y. Zhou, G. Wang and S. S. Xie, *J. Phys. Chem. B*, 2004, **108**, 10751-10753.

25. W. W. Zhou, L. Ding, S. Yang and J. Liu, *ACS Nano*, 2011, **5**, 3849-3857.

26. D. H. Choi, Q. Wang, Y. Azuma, Y. Majima, J. H. Warner, Y. Miyata, H. Shinohara and R. Kitaura, *Sci. Rep.*, 2013, **3**, 1617.

27. C. G. Zhang, K. Bets, S. S. Lee, Z. Z. Sun, F. Mirri, V. L. Colvin, B. I. Yakobson, J. M. Tour and R. H. Hauge, *ACS Nano*, 2012, **6**, 6023-6032.

28. J. Y. Sun, Y. B. Chen, M. K. Priydarshi, Z. Chen, A. Bachmatiuk, Z. Y. Zou, Z. L. Chen, X. J. Song, Y. F. Gao, M. H. Rummeli, Y. F. Zhang and Z. F. Liu, *Nano Lett.*, 2015, **15**, 5846-5854.